AMERICAN SOCIETY of
GENE & CELL
THERAPY

Intravenous Injection of an AAV-PHP.B Vector Encoding Human Acid α-Glucosidase Rescues Both Muscle and CNS Defects in Murine Pompe Disease

Jeong-A Lim,[1] Haiqing Yi,[1] Fengqin Gao,[1] Nina Raben,[2] Priya S. Kishnani,[1] and Baodong Sun[1]

[1]Department of Pediatrics, Division of Medical Genetics, Duke University School of Medicine, Durham, NC, USA; [2]Cell Biology and Physiology Center, National Heart, Lung, and Blood Institute, NIH, Bethesda, MD, USA

Pompe disease, a severe and often fatal neuromuscular disorder, is caused by a deficiency of the lysosomal enzyme acid alpha-glucosidase (GAA). The disease is characterized by the accumulation of excess glycogen in the heart, skeletal muscle, and CNS. Currently approved enzyme replacement therapy or experimental adeno-associated virus (AAV)-mediated gene therapy has little effect on CNS correction. Here we demonstrate that a newly developed AAV-PHP.B vector can robustly transduce both the CNS and skeletal muscles in GAA-knockout (GAAKO) mice. A single intravenous injection of an AAV-PHP.B vector expressing human GAA under the control of cytomegalovirus (CMV) enhancer-chicken β-actin (CB) promoter into 2-week-old GAAKO mice resulted in widespread GAA expression in the affected tissues. Glycogen contents were reduced to wild-type levels in the brain and heart, and they were significantly decreased in skeletal muscle by the AAV treatment. The histological assay showed no visible glycogen in any region of the brain and spinal cord of AAV-treated mice. In this study, we describe a set of behavioral tests that can detect early neurological deficits linked to extensive lysosomal glycogen accumulation in the CNS of untreated GAAKO mice. Furthermore, we demonstrate that the therapy can help prevent the development of these abnormalities.

INTRODUCTION

Pompe disease (also called acid maltase deficiency or glycogen storage disease type II) is an autosomal recessive disorder of glycogen metabolism that is caused by pathogenic mutations in the acid alpha-glucosidase (*GAA*) gene. The GAA enzyme carries out its function, the hydrolysis of glycogen to glucose, in the lysosomes. A total loss or functional deficiency of the GAA enzyme results in a buildup of glycogen within the lysosomes, leading to damage in multiple organs and tissues, particularly skeletal, cardiac, and smooth muscles.[1–3]

When the residual enzyme activity is extremely low (less than 1% normal), the disease presents soon after birth with profound muscle weakness and poor muscle tone, hypertrophic cardiomyopathy, and respiratory insufficiency. If left untreated, most babies die from cardiac failure before their first birthday. This most severe form of the disease is classified as infantile-onset Pompe disease (IOPD).[4,5] The

enzyme activity above 1% normal (up to 30%) is compatible with a less devastating clinical course. Affected individuals experience symptoms of progressive muscle weakness, which arise in early childhood, adolescence, or adulthood. This so-called milder form is classified as late-onset Pompe disease (LOPD), in which cardiac defects are usually absent. Nonetheless, muscle weakness, in particular the diaphragm, leads to serious breathing problems and respiratory failure.[2,6]

Justifiably, Pompe disease has long been considered a muscle disorder.[1,3] However, autopsy reports, dated almost half a century ago, documented abnormal glycogen accumulation in the brain and the spinal cord of Pompe disease infants.[7–9] More recent studies confirmed these findings: diffuse glycogen storage in multiple tissues, including the CNS, was detected at autopsies of individuals with IOPD[10,11] and of the affected fetus in the second trimester.[12] The clinical consequences of these abnormalities became evident because of the significant increase in life expectancy of infants due to the introduction of enzyme replacement therapy (ERT) with recombinant human GAA (rhGAA, Alglucosidase alfa). One of the greatest benefits of ERT, the only available therapy for Pompe disease, has been its sustained improvement of cardiac abnormalities and prevention of cardiac failure.[13,14] On the other hand, the limitations of ERT include poor targeting of the rhGAA to skeletal muscle, immune response to the exogenous protein (particularly harmful in those who produce no endogenous GAA), and the inability of the drug to cross the blood-brain barrier.[15,16]
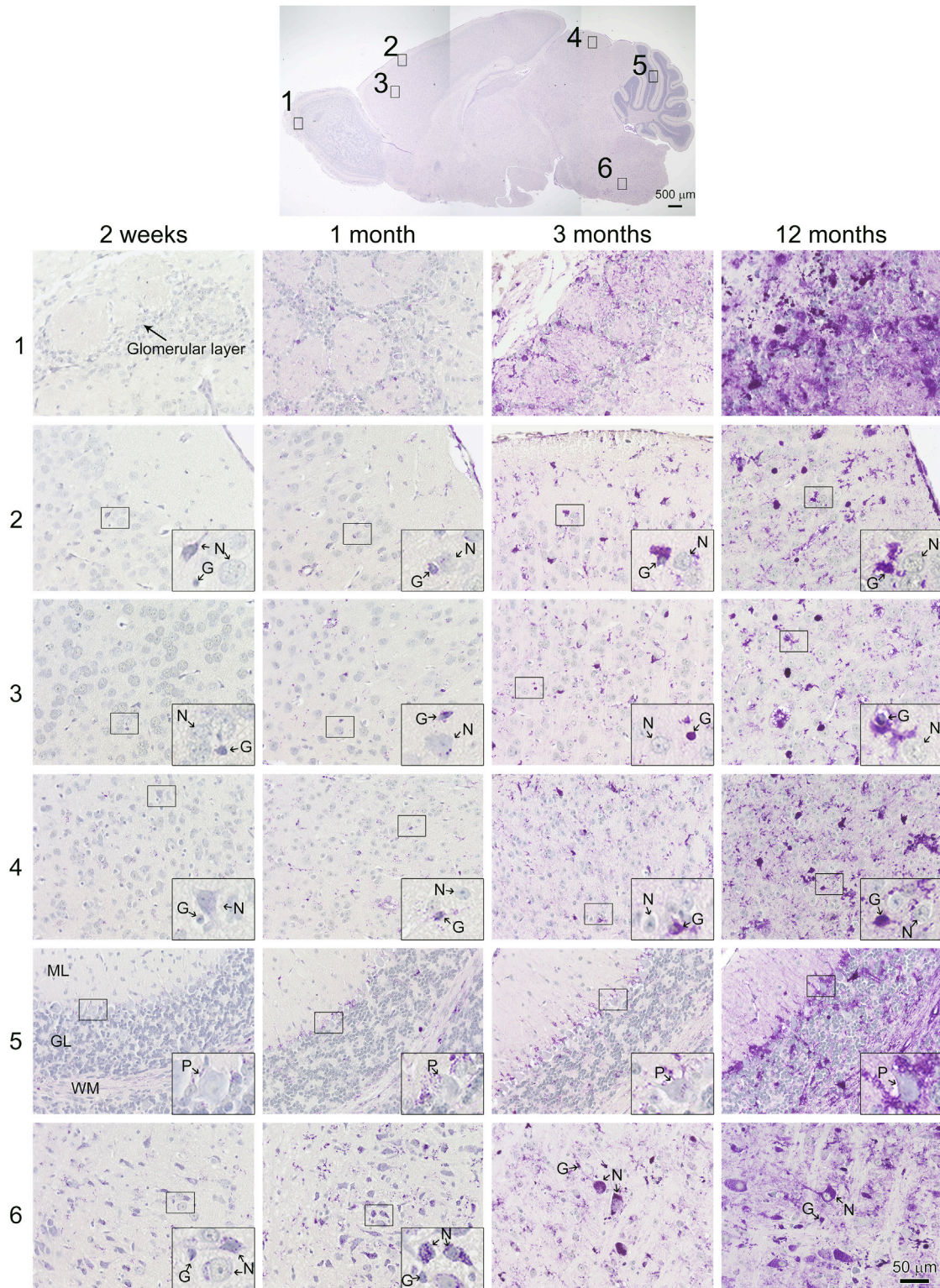
The changes brought about by ERT altered the natural course of IOPD and resulted in the emergence of a new phenotype in long-term survivors: among other symptoms, the patients suffer from gross motor and facial muscle weakness, ptosis, speech difficulties, dysphagia, orthopedic deformities, respiratory problems, and

(legend on next page)

neurological abnormalities.[17–20] A severe progressive neurodegenerative process affecting the motor neurons has been reported in an infantile patient on therapy.[21] More recent studies using brain MRI revealed slowly progressive white matter abnormalities in ERT-treated long-term survivors. Although neurophysiological tests showed overall stable cognition, learning disability is an emerging feature of the disease.[16,22,23]

The contribution of neurological deficits to the pathophysiology of the disease resulting from glycogen storage in the brain, the spinal cord, and in respiratory-related motoneurons (in particular, phrenic motoneurons) has been also highlighted in GAA-knockout (GAAKO) mice, a model of Pompe disease.[19,24–26] Complex neuropathological changes in the spinal cord of GAAKO mice were documented by genome-wide screening of mRNA expression and histological analysis.[25] Reversal of the CNS pathology in GAAKO mice was achieved by intrathecal administration of adeno-associated virus (AAV)9 or AAVrh10 vectors expressing hGAA; although muscle glycogen content was not affected by this treatment, muscle strength was partially restored, again suggesting that motor weakness in Pompe disease was not caused by muscle pathology alone.[27]

Thus, clinical findings and studies in mice underscore the need for targeting both skeletal muscle and the nervous system in Pompe disease. Here we demonstrate the feasibility of correcting the CNS and muscle defects by AAV-mediated gene therapy in GAAKO mice using a novel AAV9 variant, AAV-PHP.B.[28] Intravenous administration of an AAV-PHP.B vector expressing hGAA increases GAA activity and reduces glycogen in both types of tissues. Furthermore, we have used a much-expanded set of behavioral tests to demonstrate that motor, sensory, and cognitive abnormalities in GAAKO mice can be rescued.

RESULTS

Age-Dependent Glycogen Accumulation in the Brain and Spinal Cord of GAAKO Mice

Glycogen accumulation in the CNS of GAAKO mice has been recently reported.[19,24,27] We have expanded this study and examined the extent of glycogen storage in various regions of the brain and spinal cord of GAAKO mice at different ages. Occasional periodic acid-Schiff (PAS)-positive structures, indicative of an excess amount of glycogen, were already seen in the cerebral cortex, midbrain, hindbrain, and cerebellum at 2 weeks of age. At 1 month of age, moderate glycogen accumulation was observed in all regions of the brain. By 3 months of age, there was a striking increase in the amount of accumulated glycogen, and by 12 months the pathology could be characterized as extensive (Figure 1). Glycogen was detected in both neuronal and glial cells; the latter appear to accumulate more glycogen than the former (Figure 1, insets) in most regions of the

brain, with the exception of the hindbrain, where both cell types seemed to have equal glycogen load (Figure 1, insets of area 6). Notably, massive glycogen accumulation was detected in the glomerular layer in the olfactory bulbs, the Purkinje cell layer, white matter in the cerebellum, and the hindbrain. Also, the coronal sections of the corpus callosum and hippocampus area from 6-month-old GAAKO mice showed intense glycogen staining (Figure S1). Similar to what was observed in the brain, PAS-positive structures were present in the spinal cord at 2 weeks of age and continued to grow with age; glycogen accumulation was most prominent in the neurons in the gray matter (Figure 2).

AAV-PHP.B-GAA-Mediated Glycogen Clearance in the CNS and Skeletal Muscle of GAAKO Mice

For systemic delivery of the *GAA* transgene, we chose the AAV-PHP.B vector that was previously shown to have high transduction efficiency in mice.[28,29] The 2-week-old GAAKO male mice were intravenously injected with the AAV-PHP.B-GAA vector at a dose of 5×10^{12} vg/kg (GAAKO-AAV), and the analysis was performed after 14 weeks. Age-matched untreated mice were used as controls (GAAKO-UT). AAV vector DNA in tissues was quantified by qPCR. The AAV copy number was high in the brain (4.82 ± 2.05), heart (6.38 ± 0.75), and liver (3.04 ± 0.60) and low but detectable in skeletal muscles (≤ 0.05) (Figure 3A). Exogenously expressed GAA protein was detected by western blotting in these tissues (Figure 3B).

Next, we assessed GAA activities and glycogen levels in tissues from wild-type (WT), AAV-treated (GAAKO-AAV), and untreated (GAAKO-UT) mice. The enzyme activity increased significantly in all tissues of the AAV-treated mice, reaching WT levels in the brain and skeletal muscles and exceeding WT levels in the heart (20-fold of WT) and liver (2.3-fold of WT) (Figure 3C). Glycogen contents were reduced to WT levels in the brain, heart, and quadriceps, and they were significantly reduced in the gastrocnemius muscle of the AAV-treated GAAKO mice (Figure 3D). Consistent with measured glycogen levels, PAS-stained tissue sections from the AAV-treated GAAKO mice showed that all regions of the brain and spinal cord were free from PAS-positive structures (Figure 4); glycogen was completely cleared in the heart and tongue, and it was markedly reduced in the gastrocnemius and diaphragm (Figure 5).

The effect of AAV-mediated gene therapy was also evaluated in GAAKO female mice. The outcome of the therapy was similar to that in GAAKO males (Figure S2). As expected, the levels of creatine kinase (CK) activity were increased in untreated GAAKO mice. In contrast, the enzyme activity was significantly reduced in AAV-treated compared to untreated GAAKO and reached WT levels

Figure 1. Age-Dependent Glycogen Accumulation in the Brain of GAAKO Mice
Paraffin-embedded sagittal sections of the brain from GAAKO mice at different ages were stained with Schiff's reagent (see the Materials and Methods) for the detection of glycogen. The images were taken from the following various brain regions: olfactory bulb (1), cerebral cortex (2 and 3), midbrain (4), cerebellum (5), and hindbrain (6). Arrows in the insets point to glial cells (G) and neurons (N). PAS staining shows progressive accumulation of glycogen (purple) in the glomerular layer of the olfactory bulb, the Purkinje cell layer, and white matter of the cerebellum and in both neuronal and glial cells of the hindbrain. ML, molecular layer; WM, white matter; GL, granular layer; P, Purkinje cell.
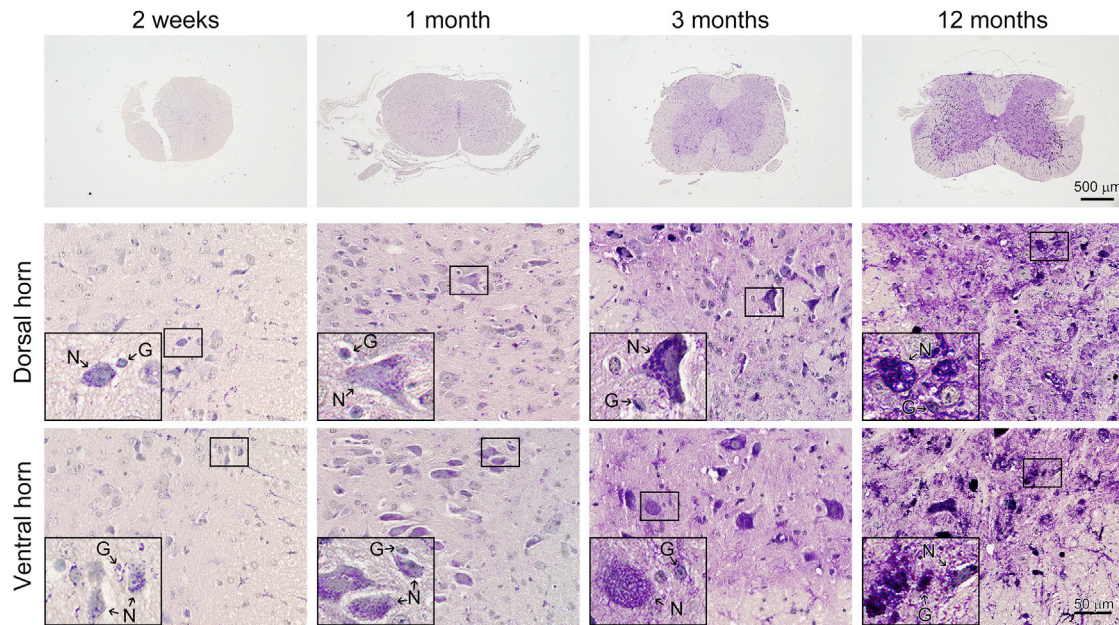
Figure 2. Age-Dependent Glycogen Accumulation in the Spinal Cord of GAAKO Mice

Paraffin-embedded sections of the spinal cord from GAAKO mice at different ages were stained with Schiff's reagent for the detection of glycogen. The images of both dorsal and ventral horn show progressive accumulation of glycogen in both glial cells (G) and neurons (N), particularly in the gray matter (GM).

(Figure S3). Taken together, these data suggest that the AAV-PHP.B-mediated gene delivery of hGAA to GAAKO mice can reverse glycogen accumulation in the CNS (where the pathology was already detectable at the start of therapy) and prevent its further buildup.

The immune response to the introduced hGAA is a major concern for the ERT and AAV-mediated gene therapy for Pompe disease. Therefore, we examined the titers of anti-hGAA antibody using ELISA at 9 and 14 weeks after the AAV administration. As shown in Figure S4, anti-hGAA antibodies were not detectable in the plasma from the AAV-treated GAAKO mice 14 weeks following the AAV administration. Thus, the successful transduction was achieved without the induction of neutralizing antibody against hGAA when mice were treated at a young age. In addition, no obvious signs of inflammation were observed by immunostaining with inflammatory marker TNF-α (tumor necrosis factor α) (Figure S5).

Prevention of Autophagic Buildup in Skeletal Muscle

The accumulation of autophagic debris in skeletal muscle is a well-established secondary abnormality stemming from the lysosomal dysfunction in Pompe disease.[30,31] As expected, skeletal muscle of untreated GAAKO mice at 4 months of age contained typical autophagic buildup, as shown by immunostaining of isolated muscle fibers with autophagic marker microtubule-associated protein 1A/1B-light chain 3 (LC3) and lysosomal marker lysosomal-associated membrane protein 1 (LAMP1) (Figure 6A, arrows). Remarkably, autophagic buildup was not seen in the fibers from the AAV-treated mice (Figure 6A). Consistent with PAS staining results, the size of lysosomes was manifestly reduced in the AAV-treated muscle, as shown by the dot-like

shape of LAMP1-positive structures (Figure 6A). The reduction of autophagic buildup by the AAV treatment was also confirmed by western blotting, showing a marked decrease in the levels of the autophagy markers LC3 and p62 (sequestosome 1 [SQSTM1])[32,33] (Figure 6B). Thus, early intervention prevents the development of detrimental autophagic buildup.

Improvement of Neurological Functions in GAAKO-AAV Mice

To establish the association of glycogen accumulation in the CNS with neurological deficits and to assess the effect of therapy, we performed a plethora of behavioral tests to evaluate motor coordination and balance, sensory impairment, and cognition in WT, untreated, and AAV-treated GAAKO mice at 4 months of age.

The cylinder test, rotarod test, beam walking, and footprint were used for assessing coordination and balance. The cylinder test is a sensitive and easy neurological test to detect spontaneous forelimb asymmetry; this test has been routinely used to evaluate motor coordination in stroke models.[34,35] An affected mouse often shows asymmetric forelimb usage while rearing within an open-top transparent cylinder. The percentage of one forepaw contact (asymmetric forelimb use) was significantly higher in the untreated GAAKO than in the WT, but it lowered to near WT level in the AAV-treated mice (Figure 7A; see also Video S1). The rotarod test is widely used to assess motor coordination and balance in mice.[35] The rotarod time (latency to fall) was significantly decreased in the untreated GAAKO compared to the WT, but it became almost indistinguishable from WT controls after the AAV treatment (Figure 7B; see also Video S2). The beam-walking test, which measures the time spent to cross a narrow beam from one end to the other,[36] also showed an impairment in
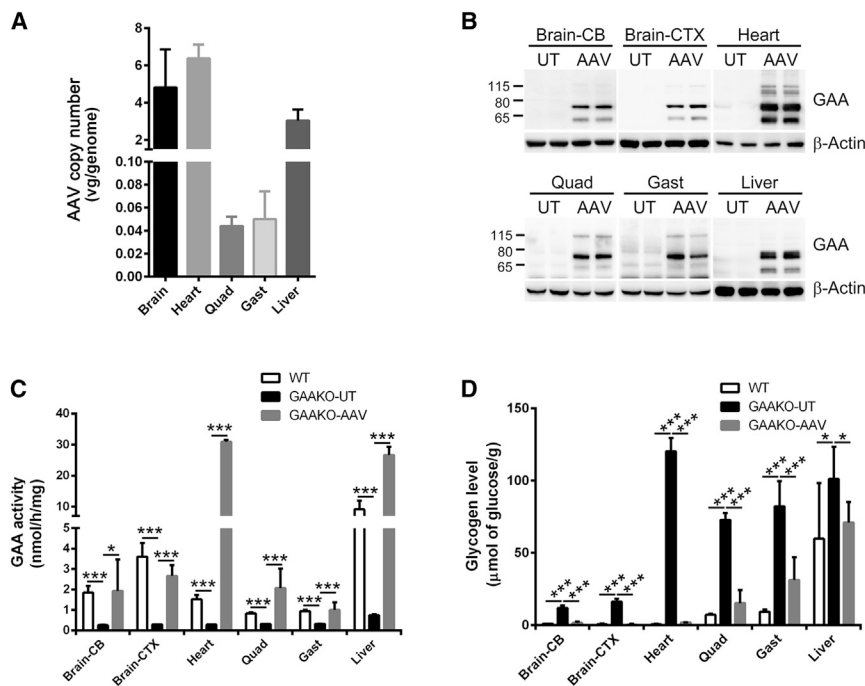
Figure 3. AAV-PHP.B-GAA Increases GAA Activity and Reduces Glycogen in Various Tissues of GAAKO Mice

AAV-PHP.B-GAA was injected intravenously into 2-week-old GAAKO mice (AAV) at a dose of 5×10^{12} vg/kg. Tissues were analyzed 14 weeks after the injection. Age-matched untreated GAAKO mice (UT) were used as controls. (A) AAV genome copy number was assessed by qPCR using hGAA primers. The graph shows the relative copy number in various tissues. Data represent mean ± SD (n = 3). (B) Western blot using anti-hGAA antibody confirmed the expression of GAA in all tissues examined; β-Actin was used as a loading control. (C and D) The treatment increased GAA activity (C) and decreased glycogen levels (D) in all tissues. CB, cerebellum; CTX, cerebral cortex; Quad, quadriceps; Gast, gastrocnemius; UT, untreated; AAV, AAV-PHP.B-GAA-treated mice. Data represent mean ± SD. *p < 0.05, ***p < 0.001. WT (n = 3), GAAKO-UT (n = 7), and GAAKO-AAV (n = 5) for the brain and heart; WT (n = 4), GAAKO-UT (n = 8), and GAAKO-AAV (n = 8) for skeletal muscles and liver.

the untreated GAAKO mice compared to the AAV-treated or WT mice (Figure 7C; see also Videos S3 and S4). Gait impairment resulting from neuromuscular defect is a typical manifestation in patients with Pompe disease.[37] Wadding gait caused by severe muscle atrophy was also reported in aged GAAKO mice.[38] To examine early gait abnormalities in GAAKO mice, we used a footprint assay to record the walking patterns and measure the distance between the fore and hind paws. The untreated GAAKO mice showed abnormal walking patterns (such as foot drag and missteps) and reduced fore-to-hind paw distance compared to WT mice; in contrast, the AAV-treated GAAKO mice showed a gait pattern similar to that in WT mice (Figures 7D and 7E).

The von Frey test (pain test) was performed to assess the sensory impairment (peripheral neuropathy) using von Frey filaments. The test measures mechanical sensitivity based on the thresholds of hind paw withdrawal in response to the filament stimulus using up and down method.[39] The withdrawal threshold increased dramatically in the untreated GAAKO mice (severe sensory impairment) compared to the WT mice, but it returned to near normal in AAV-treated mice (Figure 7F). Finally, we evaluated cognition ability by a novel object recognition test, which is designed to assess recognition memory exploiting the natural propensity of rodents to spend more time exploring novel objects.[40,41] The untreated GAAKO spent less time exploring a novel object than did WT mice; the condition was significantly improved in the AAV-treated mice (Figure 7G).

Taken together, these testing results suggest that the accumulation of glycogen in the brain affects neurological functions in GAAKO mice

and that these abnormalities can be prevented by the AAV-PHP.B-mediated gene therapy.

DISCUSSION

Pompe disease is an autosomal recessive disorder resulting from mutations in a single gene, and as such it is an excellent candidate for gene therapy. In this study, we have applied in vivo gene therapy to rescue the metabolic and functional defects in GAAKO mice by a single administration of AAV vector containing a regulatory cassette to drive GAA expression (AAV-PHP.B- chicken β-actin [CB]-hGAA) in the heart, skeletal muscles, and CNS. Gene therapy has been an area of great interest in this illness because it offers an attractive alternative to ERT, the only FDA-approved treatment for Pompe disease patients. ERT involves lifelong intravenous infusions of a high dose, as high as 40 mg/kg/week or even twice a week, of the recombinant enzyme.[42,43] Unlike ERT, gene therapy could provide equal or better outcome while requiring only a single administration.[44]

Furthermore, the advantages of gene therapy for Pompe disease go well beyond the cost and convenience for the patients. A decade of experience with ERT has demonstrated that the recombinant enzyme fails to fully correct the pathology in skeletal muscle—a major disease-relevant tissue. This shortcoming is primarily due to the inefficient uptake and lysosomal targeting of the drug in muscle.[45,46] Persistent muscle weakness can lead to respiratory insufficiency in both IOPD and LOPD patients despite ongoing ERT.[20,47,48] Therefore, it is not surprising that the initial gene therapy approaches focused on achieving therapeutic levels of the enzyme in skeletal muscle.
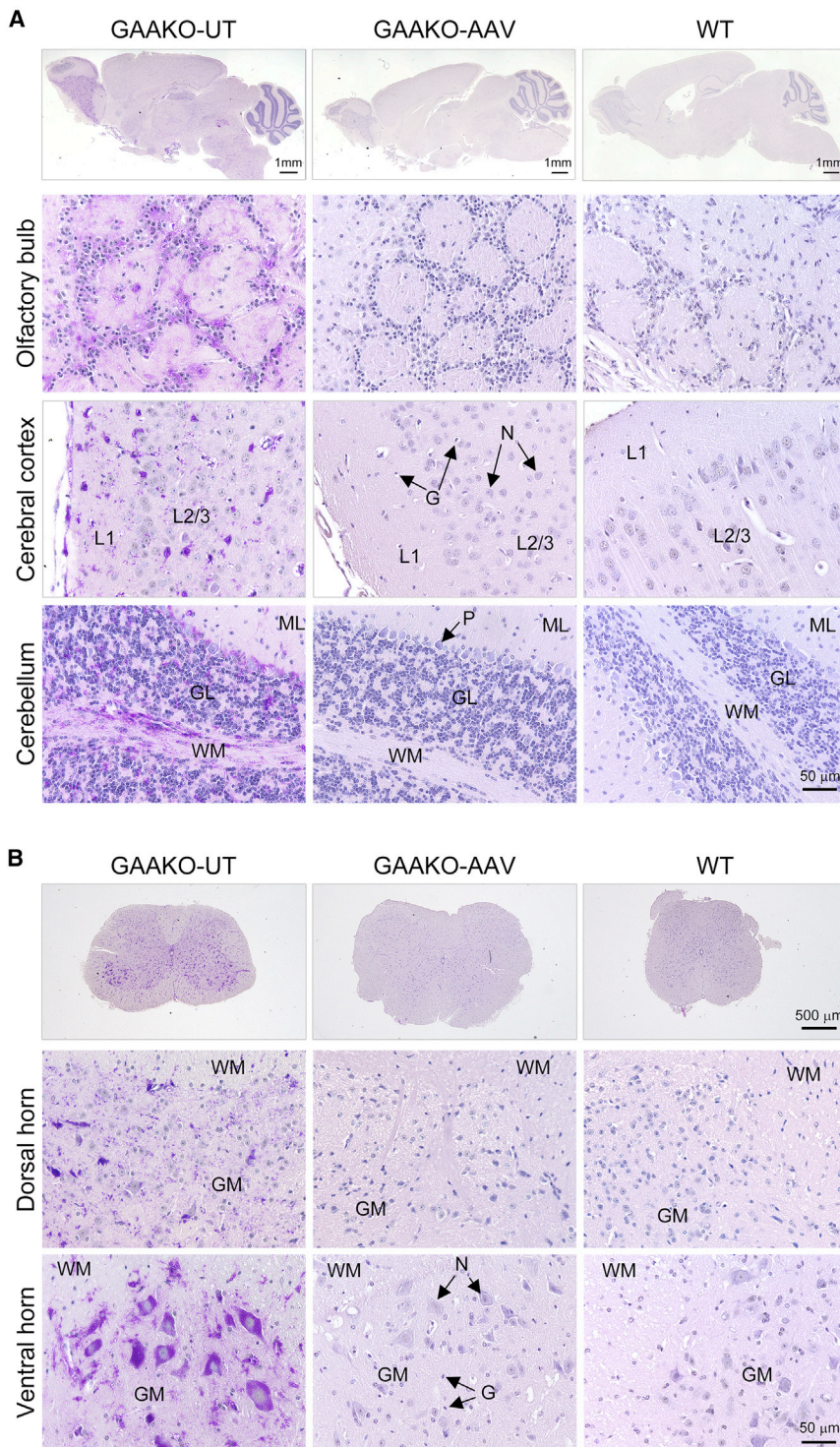
Figure 4. The Effect of AAV-PHP.B-GAA on Glycogen Storage in the CNS of GAAKO mice
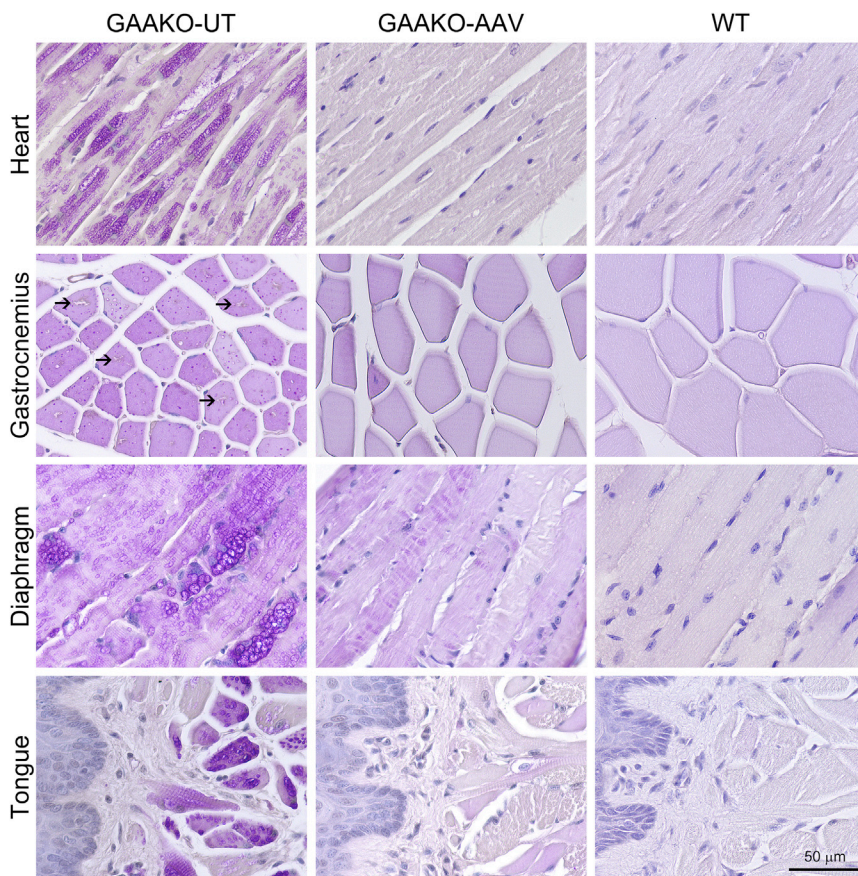
Representative images of PAS-stained sections of the brain (A) and spinal cord (B) from WT, untreated (GAAKO-UT), and AAV-PHP.B-GAA-treated GAAKO mice (GAAKO-AAV). No glycogen accumulation is seen in the glomerular layer in the olfactory bulbs, Purkinje cell layer, the white matter of the cerebellum, and the neuronal and glial cells in the spinal cord. L1, layer 1; L2-3, layer 2-3; G, glial cell; N, neuron; P, Purkinje cell; ML, molecular layer; GL, granular layer; WM, white matter; GM, gray matter.

also, unlike the WT virus, the recombinant vectors (rAAVs) do not integrate into the host genome and remain mainly episomal.[49] Multiple studies, including ours, explored muscle targeting by the direct injection of AAV vectors expressing GAA under the control of muscle-specific promoters. This approach resulted in an increased expression of GAA protein in KO mice,[50,51] but glycogen reduction was limited to the injected muscle, without metabolic cross-correction in other muscle groups. Systemic delivery of AAV vectors of different serotypes expressing hGAA driven by muscle-specific promoters yielded better, although variable, results.[51,52] AAV-mediated liver-targeted therapy has also been extensively studied in preclinical settings; high levels of liver transduction resulted in GAA secretion in the circulation and uptake by the peripheral organs, including muscle.[53–55]

As our understanding of the pathophysiology of Pompe disease has changed in recent years, it became clear that, even if muscle pathology is fully reversed, muscle weakness and respiratory problems may still persist because of the neurological deficits due to excessive glycogen accumulation in the spinal cord, particularly in phrenic motoneurons.[19,56,57] Indeed, in a series of preclinical studies, neuromuscular improvement was achieved following spinal, intrathecal, or intracerebroventricular delivery of AAV-GAA, although muscle glycogen storage remained the same as in untreated GAAKO mice.[27,58,59] The capacity of AAV for retrograde movement and transduction of phrenic motor neurons was explored in preclinical trials and in the first-in-human trial of diaphragmatic gene therapy (AAV1-cytomegalovirus [CMV]-GAA) in five children with IOPD who required assisted ventilation prior to the study.[60–63] The study demonstrated

Among different viral vectors tested in GAAKO mice, AAV has become the vector of choice for Pompe disease gene therapy because of the ability of the virus to infect both dividing and non-dividing cells and to provide high transduction efficiency in different target tissues;

Figure 5. The Effect of AAV-PHP.B-GAA on Glycogen Storage in the Muscles of GAAKO mice

Representative images of PAS-stained sections of the muscles from WT, untreated (GAAKO-UT), and AAV-PHP.B-GAA-treated GAAKO mice (GAAKO-AAV). No glycogen accumulation is seen in the heart and tongue. A decrease in the accumulation of glycogen is observed in the gastrocnemius muscle. The black arrows point to the areas of autophagic accumulation in the gastrocnemius muscle. Occasional PAS-positive structures are seen in the diaphragm from AAV-PHP.B-GAA-treated mice.

cord, and we apply several tests, including some that were never used before in this model, to evaluate both motor and cognitive changes in GAAKO mice. Importantly, we have demonstrated that the previously unrecognized early neurological abnormalities can be detected by 4 months of age. This new set of behavioral tests can be used to evaluate the effect of different therapies in GAAKO mice. Perhaps, no less important, we have shown that these neurological abnormalities can be prevented by the CNS-targeted gene therapy.

The AAV vector we chose for the study was a novel variant isolated from a library of AAV9-derived capsids, called PHP.B, which was recently shown to have high transduction efficiency in the CNS after intravenous injection.[28] However, more recent studies indicated that this exceptionally high CNS tropism of PHB.P capsid appears to be limited to the transgenic mouse model (Cre transgenic mouse on a C57BL/6J background) in which it was selected; the enhanced blood-brain barrier (BBB) penetrance of AAV-PHP.B was not replicated in other mouse strains.[65] In non-human primates, the CNS transduction efficiency was also comparable between the PHP.B and original AAV9 vectors, except for the peripheral dorsal root ganglia neurons, in which the effect of AAV-PHP.B was more pronounced.[66]

Nonetheless, the transduction efficiency of PHB.P-CB-hGAA was high enough to prevent glycogen accumulation in the brain of GAAKO mice and to rescue the associated neurological phenotype. The copy number in skeletal muscle was lower than in other tissues, but the therapeutic levels of GAA activity were achieved, leading to the correction of muscle pathology. GAA activity was particularly high in the heart of AAV-treated GAAKO mice without causing obvious toxicity. It is well established that cardiac muscle responds well to ERT; however, recent research indicated that, although cardiac failure is no longer the cause of death in IOPD on ERT, the long-term survivors are still at risk of cardiac rhythm disturbances,[67] suggesting that gene therapy may outperform ERT in preventing cardiovascular complications.[68]

the safety of the AAV treatment and resulted in modest therapeutic benefits.

The approach we used to deliver the transgene to GAAKO mice reflects the most currently held view that the reversal of the pathology in the heart, skeletal muscle, and CNS is necessary for the phenotypic correction in Pompe disease. Progressive accumulation of glycogen in the brain of infantile patients was known for decades, but the clinical consequences of the pathology did not seem particularly important because the patients suffered from severe cardiac and muscle abnormalities and most died before 1 year of age. The circumstances changed dramatically with the introduction of ERT; the neurological and cognitive aspects came to light in long-term survivors with IOPD, many of whom are now in their teens.[16] Given the persistence of muscle involvement, the assessment of the cognitive abilities in ERT-treated children and youngsters with IOPD is a challenging task. Our own studies on the developmental and academic outcomes in a group of adolescents with IOPD emphasize the variability among the patients, and they suggest a learning rather than intellectual disability in long-term survivors.[64]
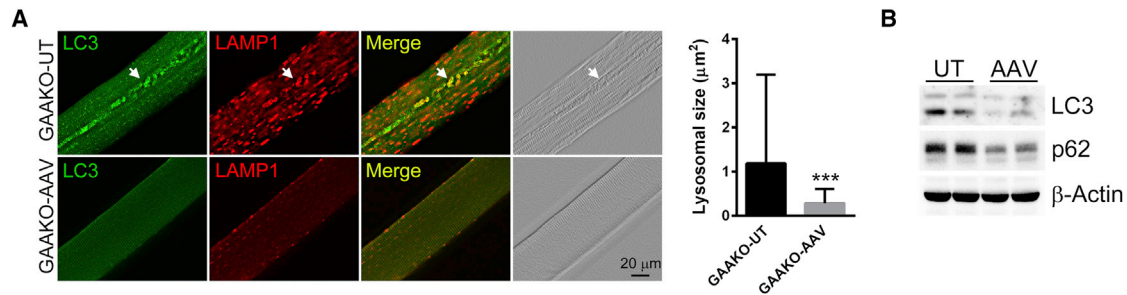
In this study, we provide morphological evidence of progressive glycogen accumulation in different regions of the brain and spinal

Figure 6. The Effect of AAV-PHP.B-GAA on Autophagy in the Skeletal Muscle of GAAKO Mice

(A) Representative images of single muscle fibers from untreated (GAAKO-UT) and AAV-PHP.B-GAA-treated GAAKO mice (GAAKO-AAV); the fibers were isolated from gastrocnemius muscle and stained with autophagic marker LC3 (green) and lysosomal marker LAMP1 (red). White arrows point to a typical autophagic buildup in myofibers from untreated GAAKO mice. LC3-negative and LAMP1-positive dot-like structures are seen in fibers from GAAKO-AAV; this pattern is a commonly recognized characteristic of the wild-type fibers.[85–87] The size of the lysosomes was measured and represented with the graph. Data represent mean ± SD. ***p < 0.001; n = 30 for GAAKO-UT fibers; n = 50 for GAAKO-AAV fibers. (B) Representative images of western blot analyses of whole-muscle lysates with the indicated antibodies. Consistent with immunostaining results, the levels of LC3 and p62 (SQSTM) (an autophagic substrate) decreased significantly in AAV-PHP.B-GAA-treated gastrocnemius muscle. β-Actin was used as a loading control.

Apart from the inability to cross the BBB, the efficacy of ERT is negatively affected by the immune responses provoked by the therapeutic enzyme. High antibody titers are inevitably associated with clinical decline and even death.[69,70] Similarly, an immune response against the expressed vector-encoded GAA poses a challenge for gene therapy. By harnessing the unique tolerogenic properties of the liver, we and others explored the benefits of liver-targeted gene therapy with or without ERT.[54,55,71] Indeed, immunotolerance was established in adult GAAKO mice following the administration of AAV vector carrying the hGAA transgene under the control of a liver-specific promoter (AAV-LSP-hGAA); in contrast, AAV vector carrying hGAA under the control of the ubiquitous CMV enhancer/CB promoter (AAV-CB-hGAA) failed to induce immunotolerance, but a significant therapeutic benefit could be achieved by co-administration of the tolerogenic AAV8-LSP-hGAA and immunogenic AAV8-CB-hGAA vectors.[72,73] These data underscore a major challenge facing the development of a gene therapy for genetic disorders, including Pompe disease: how to attain the therapeutic levels of transduction in the target tissues while preventing immune responses. In our study, we succeeded in both by initiating the therapy in young (2-week-old) GAAKO mice by using AAV-PHP.B-CB-hGAA, which allowed for efficient transduction in the heart, skeletal muscle, and CNS, leading to the correction of biochemical defects and to the phenotypic rescue.

MATERIALS AND METHODS

AAV Vector Production

The AAV-PHP.B capsid plasmid was a gift from Dr. Benjamin Deverman of the California Institute of Technology.[28] The AAV-CB-hGAA vector[74] containing a universal CMV enhancer/CB) hybrid promoter, the hGAA cDNA, and the human growth hormone polyadenylation sequence was packaged as AAV-PHP.B in HEK293T cells using phosphate-mediated transfection; the viral vector was purified using the iodixanol gradient ultracentrifugation method.[75] The titer of the viral stock was determined using purified viral DNA and Southern blotting with a biotin-labeled probe generated with Prime-A-Gene labeling kit

(Promega, Madison, WI, USA). The viral vector stock was handled according to Biohazard Safety Level 2 guidelines published by the NIH.

Animals and Virus Administration

Animal care and experiments were conducted in accordance with Duke University Institutional Animal Care and Use Committee-approved guidelines. The 2-week-old male GAAKO[76] mice received a single intravenous (via the retro-orbital sinus) injection of the AAV-PHP.B-GAA vector at a dose of 5×10^{12} vector genome (vg)/kg. Gender- and age-matched untreated GAAKO and C57BL/6J WT (from Jackson Laboratory) mice were included as controls. All mice were tested for functional performance and then sacrificed at 4 months of age (14 weeks after the AAV injection) to collect tissues and blood. Fresh tissue specimens were either immediately frozen on dry ice and stored at −80°C until use for biochemical analyses or fixed for histology.

AAV Copy Number Determination

DNA was extracted from frozen tissues using the Wizard Genomic DNA Purification kit (Promega, Madison, WI, USA). Real-time qPCR was performed using SYBR Green (Roche, Basel, Switzerland) primer pairs 5′-AGTGCCCACACAGTGCGACGT-3′ and 5′-CCTC GTAGCGCCTGTTAGCTG-3′ for hGAA and 5′-AGAGGGAAATC GTGCGTGAC-3′ and 5′-CAATAGTGATGACCTGGCCGT-3′ for mouse β-actin.[74] The AAV-CB-GAA plasmid DNA was used to generate the standard curve for viral vector copy number calculation.

PAS Staining

Sections of paraffin-embedded tissues were PAS stained as described,[77,78] with some modifications. Briefly, non-muscle tissues were fixed in 10% neutral-buffered formalin (NBF) for 48 h. After primary immersion fixation, the samples were post-fixed with 1% periodic acid (PA) in 10% NBF for 48 h at 4°C. The samples were then washed with PBS, dehydrated with ascending grades of alcohol, cleared with xylene, and infiltrated with paraffin. Gastrocnemius
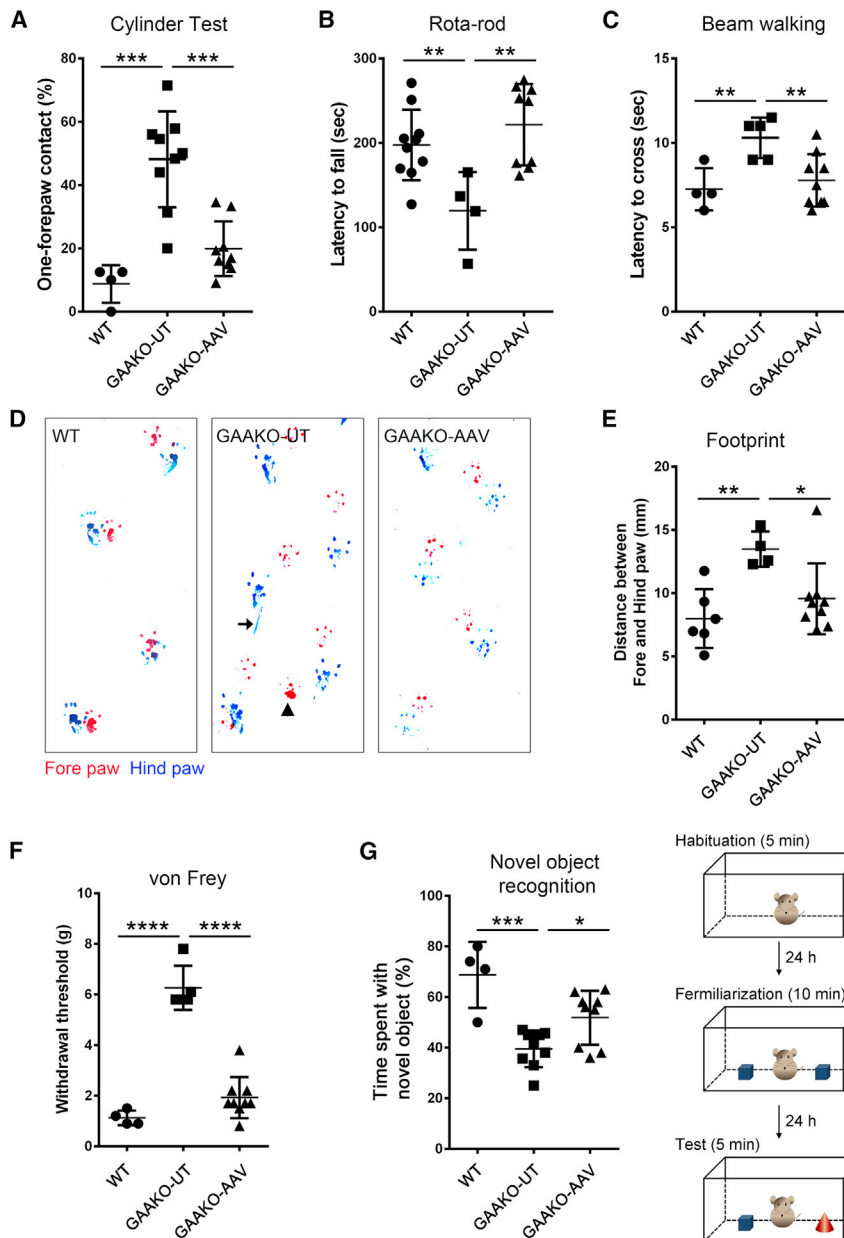
Figure 7. The Effect of AAV-PHP.B-GAA on Behavioral Defects in GAAKO Mice

Motor coordination and balance were assessed by the cylinder (A; see also Videos S1 and S2), beam walking (B; see also Videos S3 and S4), rotarod (C), and footprint tests (D and E). The percentage of one-fore paw contacts in the cylinder test, the latency to traverse beam, and the distance between fore (red) and hind (blue) paws in the footprint test were significantly lower (reaching the WT levels) in GAAKO-AAV compared to GAAKO-UT mice. The latency to fall off the rotarod increased to the WT levels and was significantly higher in treated mice compared to untreated animals. (F) The sensory defect was evaluated by the von Frey test. The hind paw withdrawal threshold was dramatically increased in GAAKO mice but returned to the WT level following AAV-PHP.B-GAA treatment. (G) The cognitive impairment was measured by the object recognition memory test. The cartoon shows the experimental design. The percentage of time spent with the novel object was significantly lower in the GAAKO compared to the WT mice; the performance improved in GAAKO-AAV mice. All the performance tests were conducted at 4 months of age. Data represent mean ± SD. Each dot indicates one individual mouse. *p < 0.05, **p < 0.01, ***p < 0.001, ****p < 0.0001. UT, untreated; AAV, AAV-PHP.B-GAA treated.

Western Blot

Tissues were homogenized on ice in RIPA buffer (PBS containing 1% NP40, 0.5% sodium deoxycholate, 0.1% SDS, and a protease and phosphatase inhibitor cocktail [Cell Signaling Technology, Danvers, MA, USA]) using a glass homogenizer. Lysates were cleared by centrifugation at 18,000 × g at 4°C for 15 min. The protein concentration of the supernatants was measured using the bicinchoninic acid (BCA) assay. Equal amounts of protein were run on SDS-PAGE gels and transferred to nitrocellulose membrane. The membranes were blocked in 3% BSA in phosphate buffered saline with Tween 20 (PBST), incubated with primary antibodies overnight at 4°C, washed, incubated with secondary antibodies, washed again, and developed using an ECL kit (Bio-Rad, Hercules, CA, USA). The images were obtained by the image analyzer (Bio-Rad, Hercules, CA, USA). The following antibodies were used: anti-LC3B (L7543) and anti-β-Actin (A3854) were from Sigma-Aldrich (St. Louis, MO, USA), and anti-SQSTM1 (ab56416) was from Abcam (Cambridge, MA, USA).

GAA Activity and Glycogen Assay

GAA activity assay was performed using 4-methylumbellifery-α-D-glucoside (4-MU) as described.[79] Briefly, tissues were homogenized in distilled water (1 mg/20 μL water) using a homogenizer, followed

muscle was fixed in 3% glutaraldehyde in 0.2 M sodium cacodylate buffer for 24 h, washed with 0.1 M sodium cacodylate buffer, and processed the same way as the post-fixed non-muscle tissues. Sections of paraffin-embedded samples (5-μm thickness) were deparaffinized and re-hydrated. The slides were oxidized with freshly made 0.5% PA for 5 min and rinsed with distilled water for 1 min. The slides were then stained with Schiff reagent for 15 min and washed with tap water for 10 min. The slides were counterstained with hematoxylin and rinsed with tap water, incubated with bluing reagent for 1 min, dehydrated, and mounted. The images were taken on a BZ-X710 microscope (Keyence America, Itasca, IL, USA). The images represent four animals for each condition.

by sonication for 15 s and centrifugation at $18,000 \times g$ at 4°C for 15 min. For the GAA activity assay, 20 μL 2.2 mM 4-Methylumbellifery-α-D-glucoside (Sigma-Aldrich, St. Louis, MO, USA) in 0.2 M sodium acetate buffer (pH 4.3) was added to 10 μL of the supernatants. The mixtures were incubated for 1 h at 37°C, and the reaction was stopped by adding 0.5 M carbonate buffer (pH 10.5). Fluorescence (360 nm excitation, 465 nm emission) was measured on a victor X multilabel plate reader. 4-Methylumbelliferone (Sigma-Aldrich, St. Louis, MO, USA) was used as a standard. For measuring glycogen content, the 1:5 diluted lysates were boiled for 3 min (to inactivate endogenous enzymes) and incubated with 0.175 U/mL (final concentration in the reaction) amyloglucosidase (Sigma-Aldrich, St. Louis, MO, USA) for 90 min at 37°C. The reaction mixtures were then boiled again for 3 min to stop the reaction. 30 μL of the mixtures was incubated with 1 mL Pointe Scientific Glucose (Hexokinase) Liquid Reagents (Fisher, Hampton, NH, USA) for at least 10 min at room temperature (RT). The absorbance at 340 nm was read on a Shimadzu UV-1700 PharmaSpec UV-VIS Spectrophotometer. Protein concentration was determined by BCA assay and used to normalize the data.

Immunostaining of a Single Muscle Fiber

Muscle fixation, isolation of single fibers, and immunostaining were performed as described,[80] with some modification. Briefly, isolated gastrocnemius muscles were fixed in 4% paraformaldehyde for 1 h at RT, washed with PBS, and incubated in cold methanol for 6 min at −20°C. The samples were then rinsed again with PBS and placed in a puddle of 0.04% saponin in PBS on a Sylgard-coated plate. Fibers were gently isolated from muscle bundles under a dissecting microscope. The isolated fibers were stained with anti-LC3 (Sigma-Aldrich, St. Louis, MO, USA) and anti-LAMP1 (BD Biosciences, Franklin Lakes, NJ, USA) antibodies using a M.O.M. kit (Vector Laboratories, Burlingame, CA, USA). The images were taken on a BZ-X710 microscope (Keyence, Itasca, IL, USA).

Accelerating Rotarod Test

Mice were trained on a rotarod (ENV-577M, Med Associates, Fairfax, VT, USA) by first allowing them to stay for 3 min on the drum, which was rotating at a constant speed of four rotations per min (waiting mode). Mice were then trained twice on a gradually accelerating rotarod (4.0–40 rpm). Trained mice were then tested during three sessions using an accelerating rotarod protocol, and the latency to fall was recorded. This routine provided at least 5 min of rest between the sessions.

Cylinder Test

Mice were placed in an 800-mL glass beaker and the vertical exploring movements were recorded for each animal for 3 min. A mirror was placed behind the cylinder to record all the rears (vertical movements with one or both forelimbs touching the walls of the cylinder). The number of rears during vertical exploration was recorded. Asymmetry in spontaneous forelimb usage was calculated by the ratio of one-to-both forelimb usage.

von Frey Test

The von Frey test was performed as described,[39,81] with minor modifications. von Frey filament was applied to walking pads for at least 5 s, and the mouse hind paw withdrawal threshold was calculated using the up and down method.[39]

Beam-Walking Test

The beam-walking test was performed as described,[82] with some modification. Briefly, mice were placed at one end of a beam (12 mm wide), and the time required to cross to the black box at the other end (800 mm away) was measured. Mice were trained twice before testing. Two successful trials in which the mouse did not stall on the beam were averaged.

Footprint Test

The footprint test was performed as described,[83] with some modification. Paws were marked with edible ink (fore paws in red and hind paws in blue), and mice were allowed to walk on a piece of white paper. Two to four steps from the middle portion of each run were measured for fore-to-hind paw distance.

Novel Object Recognition Test

The novel object recognition test was performed as described,[84] with slight modifications. Briefly, a mouse was habituated in the empty open field ($530 \times 427 \times 188$ mm) for 5 min. After 24 h, two identical objects were placed in the open field, and the mouse was allowed to familiarize with the objects for 10 min. After an additional 24 h, one of the familiar objects was replaced with a novel object. The amount of time taken to explore the new object was measured during a 5-min session, and the percentage of time spent with the novel object to total exploration time was calculated.

Statistics

Statistical significance was determined by unpaired two-tailed Student's t test using Prism software (GraphPad, La Jolla, CA, USA). Data are presented as mean ± SD; *p < 0.05 was considered statistically significant (**p < 0.01; ***p < 0.001).

SUPPLEMENTAL INFORMATION

Supplemental Information includes Supplemental Materials and Methods, five figures, and four videos and can be found with this article online at https://doi.org/10.1016/j.omtm.2019.01.006.

AUTHOR CONTRIBUTIONS

CONFLICTS OF INTEREST

REFERENCES

1. Hirschhorn, R., and Reuser, A.J. (2001). Glycogen Storage Disease Type II: Acid alpha Glucosidase (Acid Maltase) Deficiency: The Metabolic and Molecular Basis of Inherited Disease (McGraw-Hill), pp. 3389–3420.

2. van der Ploeg, A.T., and Reuser, A.J. (2008). Pompe's disease. Lancet 372, 1342–1353.

3. Pauly, D.F., Fraites, T.J., Toma, C., Bayes, H.S., Huie, M.L., Hirschhorn, R., Plotz, P.H., Raben, N., Kessler, P.D., and Byrne, B.J. (2001). Intercellular transfer of the virally derived precursor form of acid alpha-glucosidase corrects the enzyme deficiency in inherited cardioskeletal myopathy Pompe disease. Hum. Gene Ther. 12, 527–538.

4. van den Hout, H.M., Hop, W., van Diggelen, O.P., Smeitink, J.A., Smit, G.P., Poll-The, B.T., Bakker, H.D., Loonen, M.C., de Klerk, J.B., Reuser, A.J., and van der Ploeg, A.T. (2003). The natural course of infantile Pompe's disease: 20 original cases compared with 133 cases from the literature. Pediatrics 112, 332–340.

5. Kishnani, P.S., Hwu, W.L., Mandel, H., Nicolino, M., Yong, F., and Corzo, D.; Infantile-Onset Pompe Disease Natural History Study Group (2006). A retrospective, multinational, multicenter study on the natural history of infantile-onset Pompe disease. J. Pediatr. 148, 671–676.

6. Van der Beek, N.A., Hagemans, M.L., Reuser, A.J., Hop, W.C., Van der Ploeg, A.T., Van Doorn, P.A., and Wokke, J.H. (2009). Rate of disease progression during long-term follow-up of patients with late-onset Pompe disease. Neuromuscul. Disord. 19, 113–117.

7. Mancall, E.L., Aponte, G.E., and Berry, R.G. (1965). Pompe's Disease (Diffuse Glycogenosis) with Neuronal Storage. J. Neuropathol. Exp. Neurol. 24, 85–96.

8. Gambetti, P., DiMauro, S., and Baker, L. (1971). Nervous system in Pompe's disease. Ultrastructure and biochemistry. J. Neuropathol. Exp. Neurol. 30, 412–430.

9. Martin, J.J., de Barsy, T., van Hoof, F., and Palladini, G. (1973). Pompe's disease: an inborn lysosomal disorder with storage of glycogen. A study of brain and striated muscle. Acta Neuropathol. 23, 229–244.

10. Martini, C., Ciana, G., Benettoni, A., Katouzian, F., Severini, G.M., Bussani, R., and Bembi, B. (2001). Intractable fever and cortical neuronal glycogen storage in glycogenosis type 2. Neurology 57, 906–908.

11. Pena, L.D., Proia, A.D., and Kishnani, P.S. (2015). Postmortem Findings and Clinical Correlates in Individuals with Infantile-Onset Pompe Disease. JIMD Rep. 23, 45–54.

12. Chen, C.P., Lin, S.P., Tzen, C.Y., Tsai, F.J., Hwu, W.L., and Wang, W. (2004). Detection of a homozygous D645E mutation of the acid alpha-glucosidase gene and glycogen deposition in tissues in a second-trimester fetus with infantile glycogen storage disease type II. Prenat. Diagn. 24, 231–232.

13. Kishnani, P.S., Corzo, D., Nicolino, M., Byrne, B., Mandel, H., Hwu, W.L., Leslie, N., Levine, J., Spencer, C., McDonald, M., et al. (2007). Recombinant human acid [alpha]-glucosidase: major clinical benefits in infantile-onset Pompe disease. Neurology 68, 99–109.

14. Kishnani, P.S., Corzo, D., Leslie, N.D., Gruskin, D., Van der Ploeg, A., Clancy, J.P., Parini, R., Morin, G., Beck, M., Bauer, M.S., et al. (2009). Early treatment with alglucosidase alpha prolongs long-term survival of infants with Pompe disease. Pediatr. Res. 66, 329–335.

15. Macauley, S.L., and Sands, M.S. (2009). Promising CNS-directed enzyme replacement therapy for lysosomal storage diseases. Exp. Neurol. 218, 5–8.

16. Ebbink, B.J., Poelman, E., Aarsen, F.K., Plug, I., Régal, L., Muentjes, C., van der Beek, N.A.M.E., Lequin, M.H., van der Ploeg, A.T., and van den Hout, J.M.P. (2018). Classic infantile Pompe patients approaching adulthood: a cohort study on consequences for the brain. Dev. Med. Child Neurol. 60, 579–586.

17. Prater, S.N., Banugaria, S.G., DeArmey, S.M., Botha, E.G., Stege, E.M., Case, L.E., Jones, H.N., Phornphutkul, C., Wang, R.Y., Young, S.P., and Kishnani, P.S. (2012). The emerging phenotype of long-term survivors with infantile Pompe disease. Genet. Med. 14, 800–810.

18. van Gelder, C.M., van Capelle, C.I., Ebbink, B.J., Moor-van Nugteren, I., van den Hout, J.M., Hakkesteegt, M.M., van Doorn, P.A., de Coo, I.F., Reuser, A.J., de Gier, H.H., and van der Ploeg, A.T. (2012). Facial-muscle weakness, speech disorders and dysphagia are common in patients with classic infantile Pompe disease treated with enzyme therapy. J. Inherit. Metab. Dis. 35, 505–511.

19. DeRuisseau, L.R., Fuller, D.D., Qiu, K., DeRuisseau, K.C., Donnelly, W.H., Jr., Mah, C., Reier, P.J., and Byrne, B.J. (2009). Neural deficits contribute to respiratory insufficiency in Pompe disease. Proc. Natl. Acad. Sci. USA 106, 9419–9424.

20. Hahn, A., Praetorius, S., Karabul, N., Dießel, J., Schmidt, D., Motz, R., Haase, C., Baethmann, M., Hennermann, J.B., Smitka, M., et al. (2015). Outcome of patients with classical infantile pompe disease receiving enzyme replacement therapy in Germany. JIMD Rep. 20, 65–75.

21. Burrow, T.A., Bailey, L.A., Kinnett, D.G., and Hopkin, R.J. (2010). Acute progression of neuromuscular findings in infantile Pompe disease. Pediatr. Neurol. 42, 455–458.

22. Ebbink, B.J., Poelman, E., Plug, I., Lequin, M.H., van Doorn, P.A., Aarsen, F.K., van der Ploeg, A.T., and van den Hout, J.M. (2016). Cognitive decline in classic infantile Pompe disease: An underacknowledged challenge. Neurology 86, 1260–1261.

23. McIntosh, P.T., Hobson-Webb, L.D., Kazi, Z.B., Prater, S.N., Banugaria, S.G., Austin, S., Wang, R., Enterline, D.S., Frush, D.P., and Kishnani, P.S. (2018). Neuroimaging findings in infantile Pompe patients treated with enzyme replacement therapy. Mol. Genet. Metab. 123, 85–91.

24. Sidman, R.L., Taksir, T., Fidler, J., Zhao, M., Dodge, J.C., Passini, M.A., Raben, N., Thurberg, B.L., Cheng, S.H., and Shihabuddin, L.S. (2008). Temporal neuropathologic and behavioral phenotype of 6neo/6neo Pompe disease mice. J. Neuropathol. Exp. Neurol. 67, 803–818.

25. Turner, S.M.F., Falk, D.J., Byrne, B.J., and Fuller, D.D. (2016). Transcriptome assessment of the Pompe (Gaa-/-) mouse spinal cord indicates widespread neuropathology. Physiol. Genomics 48, 785–794.

26. Turner, S.M., Hoyt, A.K., ElMallah, M.K., Falk, D.J., Byrne, B.J., and Fuller, D.D. (2016). Neuropathology in respiratory-related motoneurons in young Pompe (Gaa(-/-)) mice. Respir. Physiol. Neurobiol. 227, 48–55.

27. Hordeaux, J., Dubreil, L., Robveille, C., Deniaud, J., Pascal, Q., Dequéant, B., Pailloux, J., Lagalice, L., Ledevin, M., Babarit, C., et al. (2017). Long-term neurologic and cardiac correction by intrathecal gene therapy in Pompe disease. Acta Neuropathol. Commun. 5, 66.

28. Deverman, B.E., Pravdo, P.L., Simpson, B.P., Kumar, S.R., Chan, K.Y., Banerjee, A., Wu, W.L., Yang, B., Huber, N., Pasca, S.P., and Gradinaru, V. (2016). Cre-dependent selection yields AAV variants for widespread gene transfer to the adult brain. Nat. Biotechnol. 34, 204–209.

29. Morabito, G., Giannelli, S.G., Ordazzo, G., Bido, S., Castoldi, V., Indrigo, M., Cabassi, T., Cattaneo, S., Luoni, M., Cancellieri, C., et al. (2017). AAV-PHP.B-Mediated Global-Scale Expression in the Mouse Nervous System Enables GBA1 Gene Therapy for Wide Protection from Synucleinopathy. Mol. Ther. 25, 2727–2742.

30. Shea, L., and Raben, N. (2009). Autophagy in skeletal muscle: implications for Pompe disease. Int. J. Clin. Pharmacol. Ther. 47 (Suppl 1), S42–S47.

31. Lim, J.A., Kakhlon, O., Li, L., Myerowitz, R., and Raben, N. (2015). Pompe disease: Shared and unshared features of lysosomal storage disorders. Rare Dis. 3, e1068978.

32. Pankiv, S., Clausen, T.H., Lamark, T., Brech, A., Bruun, J.A., Outzen, H., Øvervatn, A., Bjørkøy, G., and Johansen, T. (2007). p62/SQSTM1 binds directly to Atg8/LC3 to facilitate degradation of ubiquitinated protein aggregates by autophagy. J. Biol. Chem. 282, 24131–24145.

33. Bjørkøy, G., Lamark, T., Pankiv, S., Øvervatn, A., Brech, A., and Johansen, T. (2009). Monitoring autophagic degradation of p62/SQSTM1. Methods Enzymol. 452, 181–197.

34. Schaar, K.L., Brenneman, M.M., and Savitz, S.I. (2010). Functional assessments in the rodent stroke model. Exp. Transl. Stroke Med. 2, 13.

35. Balkaya, M., Kröber, J.M., Rex, A., and Endres, M. (2013). Assessing post-stroke behavior in mouse models of focal ischemia. J. Cereb. Blood Flow Metab. 33, 330–338.

36. Stanley, J.L., Lincoln, R.J., Brown, T.A., McDonald, L.M., Dawson, G.R., and Reynolds, D.S. (2005). The mouse beam walking assay offers improved sensitivity over the mouse rotarod in determining motor coordination deficits induced by benzodiazepines. J. Psychopharmacol. (Oxford) 19, 221–227.

37. McIntosh, P.T., Case, L.E., Chan, J.M., Austin, S.L., and Kishnani, P. (2015). Characterization of gait in late onset Pompe disease. Mol. Genet. Metab. 116, 152–156.

38. Raben, N., Nagaraju, K., Lee, E., and Plotz, P. (2000). Modulation of disease severity in mice with targeted disruption of the acid alpha-glucosidase gene. Neuromuscul. Disord. 10, 283–291.

39. Dixon, W.J. (1980). Efficient analysis of experimental observations. Annu. Rev. Pharmacol. Toxicol. 20, 441–462.

40. Ennaceur, A., and Delacour, J. (1988). A new one-trial test for neurobiological studies of memory in rats. 1: Behavioral data. Behav. Brain Res. 31, 47–59.

41. Grayson, B., Leger, M., Piercy, C., Adamson, L., Harte, M., and Neill, J.C. (2015). Assessment of disease-related cognitive impairments using the novel object recognition (NOR) task in rodents. Behav. Brain Res. 285, 176–193.

42. Landis, J.L., Hyland, H., Kindel, S.J., Punnoose, A., and Geddes, G.C. (2018). Pompe disease treatment with twice a week high dose alglucoside alfa in a patient with severe dilated cardiomyopathy. Mol. Genet. Metab. Rep. 16, 1–4.

43. van Gelder, C.M., Poelman, E., Plug, I., Hoogeveen-Westerveld, M., van der Beek, N.A.M.E., Reuser, A.J.J., and van der Ploeg, A.T. (2016). Effects of a higher dose of alglucosidase alfa on ventilator-free survival and motor outcome in classic infantile Pompe disease: an open-label single-center study. J. Inherit. Metab. Dis. 39, 383–390.

44. Falk, D.J., Soustek, M.S., Todd, A.G., Mah, C.S., Cloutier, D.A., Kelley, J.S., Clement, N., Fuller, D.D., and Byrne, B.J. (2015). Comparative impact of AAV and enzyme replacement therapy on respiratory and cardiac function in adult Pompe mice. Mol. Ther. Methods Clin. Dev. 2, 15007.

45. Zhu, Y., Li, X., McVie-Wylie, A., Jiang, C., Thurberg, B.L., Raben, N., Mattaliano, R.J., and Cheng, S.H. (2005). Carbohydrate-remodelled acid alpha-glucosidase with higher affinity for the cation-independent mannose 6-phosphate receptor demonstrates improved delivery to muscles of Pompe mice. Biochem. J. 389, 619–628.

46. McVie-Wylie, A.J., Lee, K.L., Qiu, H., Jin, X., Do, H., Gotschall, R., Thurberg, B.L., Rogers, C., Raben, N., O'Callaghan, M., et al. (2008). Biochemical and pharmacological characterization of different recombinant acid alpha-glucosidase preparations evaluated for the treatment of Pompe disease. Mol. Genet. Metab. 94, 448–455.

47. Chakrapani, A., Vellodi, A., Robinson, P., Jones, S., and Wraith, J.E. (2010). Treatment of infantile Pompe disease with alglucosidase alpha: the UK experience. J. Inherit. Metab. Dis. 33, 747–750.

48. Schoser, B., Stewart, A., Kanters, S., Hamed, A., Jansen, J., Chan, K., Karamouzian, M., and Toscano, A. (2017). Survival and long-term outcomes in late-onset Pompe disease following alglucosidase alfa treatment: a systematic review and meta-analysis. J. Neurol. 264, 621–630.

49. Mingozzi, F., and High, K.A. (2011). Therapeutic in vivo gene transfer for genetic disease using AAV: progress and challenges. Nat. Rev. Genet. 12, 341–355.

50. Fraites, T.J., Jr., Schleissing, M.R., Shanely, R.A., Walter, G.A., Cloutier, D.A., Zolotukhin, I., Pauly, D.F., Raben, N., Plotz, P.H., Powers, S.K., et al. (2002). Correction of the enzymatic and functional deficits in a model of Pompe disease using adeno-associated virus vectors. Mol. Ther. 5, 571–578.

51. Sun, B., Zhang, H., Franco, L.M., Brown, T., Bird, A., Schneider, A., and Koeberl, D.D. (2005). Correction of glycogen storage disease type II by an adeno-associated virus vector containing a muscle-specific promoter. Mol. Ther. 11, 889–898.

52. Doerfler, P.A., Nayak, S., Corti, M., Morel, L., Herzog, R.W., and Byrne, B.J. (2016). Targeted approaches to induce immune tolerance for Pompe disease therapy. Mol. Ther. Methods Clin. Dev. 3, 15053.

53. Sun, B., Young, S.P., Li, P., Di, C., Brown, T., Salva, M.Z., Li, S., Bird, A., Yan, Z., Auten, R., et al. (2008). Correction of multiple striated muscles in murine Pompe disease through adeno-associated virus-mediated gene therapy. Mol. Ther. 16, 1366–1371.

54. Sun, B., Bird, A., Young, S.P., Kishnani, P.S., Chen, Y.T., and Koeberl, D.D. (2007). Enhanced response to enzyme replacement therapy in Pompe disease after the induction of immune tolerance. Am. J. Hum. Genet. 81, 1042–1049.

55. Sun, B., Kulis, M.D., Young, S.P., Hobeika, A.C., Li, S., Bird, A., Zhang, H., Li, Y., Clay, T.M., Burks, W., et al. (2010). Immunomodulatory gene therapy prevents antibody formation and lethal hypersensitivity reactions in murine pompe disease. Mol. Ther. 18, 353–360.

56. Fuller, D.D., ElMallah, M.K., Smith, B.K., Corti, M., Lawson, L.A., Falk, D.J., and Byrne, B.J. (2013). The respiratory neuromuscular system in Pompe disease. Respir. Physiol. Neurobiol. 189, 241–249.

57. Todd, A.G., McElroy, J.A., Grange, R.W., Fuller, D.D., Walter, G.A., Byrne, B.J., and Falk, D.J. (2015). Correcting Neuromuscular Deficits With Gene Therapy in Pompe Disease. Ann. Neurol. 78, 222–234.

58. Qiu, K., Falk, D.J., Reier, P.J., Byrne, B.J., and Fuller, D.D. (2012). Spinal delivery of AAV vector restores enzyme activity and increases ventilation in Pompe mice. Mol. Ther. 20, 21–27.

59. Lee, N.C., Hwu, W.L., Muramatsu, S.I., Falk, D.J., Byrne, B.J., Cheng, C.H., Shih, N.C., Chang, K.L., Tsai, L.K., and Chien, Y.H. (2018). A Neuron-Specific Gene Therapy Relieves Motor Deficits in Pompe Disease Mice. Mol. Neurobiol. 55, 5299–5309.

60. Smith, B.K., Collins, S.W., Conlon, T.J., Mah, C.S., Lawson, L.A., Martin, A.D., Fuller, D.D., Cleaver, B.D., Clément, N., Phillips, D., et al. (2013). Phase I/II trial of adeno-associated virus-mediated alpha-glucosidase gene therapy to the diaphragm for chronic respiratory failure in Pompe disease: initial safety and ventilatory outcomes. Hum. Gene Ther. 24, 630–640.

61. Byrne, P.I., Collins, S., Mah, C.C., Smith, B., Conlon, T., Martin, S.D., Corti, M., Cleaver, B., Islam, S., and Lawson, L.A. (2014). Phase I/II trial of diaphragm delivery of recombinant adeno-associated virus acid alpha-glucosidase (rAAaV1-CMV-GAA) gene vector in patients with Pompe disease. Hum. Gene Ther. Clin. Dev. 25, 134–163.

62. Smith, B.K., Martin, A.D., Lawson, L.A., Vernot, V., Marcus, J., Islam, S., Shafi, N., Corti, M., Collins, S.W., and Byrne, B.J. (2017). Inspiratory muscle conditioning exercise and diaphragm gene therapy in Pompe disease: Clinical evidence of respiratory plasticity. Exp. Neurol. 287, 216–224.

63. Corti, M., Liberati, C., Smith, B.K., Lawson, L.A., Tuna, I.S., Conlon, T.J., Coleman, K.E., Islam, S., Herzog, R.W., Fuller, D.D., et al. (2017). Safety of Intradiaphragmatic Delivery of Adeno-Associated Virus-Mediated Alpha-Glucosidase (rAAV1-CMV-hGAA) Gene Therapy in Children Affected by Pompe Disease. Hum. Gene Ther. Clin. Dev. 28, 208–218.

64. Spiridigliozzi, G.A., Keeling, L.A., Stefanescu, M., Li, C., Austin, S., and Kishnani, P.S. (2017). Cognitive and academic outcomes in long-term survivors of infantile-onset Pompe disease: A longitudinal follow-up. Mol. Genet. Metab. 121, 127–137.

65. Hordeaux, J., Wang, Q., Katz, N., Buza, E.L., Bell, P., and Wilson, J.M. (2018). The Neurotropic Properties of AAV-PHP.B Are Limited to C57BL/6J Mice. Mol. Ther. 26, 664–668.

66. Matsuzaki, Y., Konno, A., Mochizuki, R., Shinohara, Y., Nitta, K., Okada, Y., and Hirai, H. (2018). Intravenous administration of the adeno-associated virus-PHP.B capsid fails to upregulate transduction efficiency in the marmoset brain. Neurosci. Lett. 665, 182–188.

67. van Capelle, C.I., Poelman, E., Frohn-Mulder, I.M., Koopman, L.P., van den Hout, J.M.P., Régal, L., Cools, B., Helbing, W.A., and van der Ploeg, A.T. (2018). Cardiac outcome in classic infantile Pompe disease after 13 years of treatment with recombinant human acid alpha-glucosidase. Int. J. Cardiol. 269, 104–110.

68. Byrne, B.J., Falk, D.J., Pacak, C.A., Nayak, S., Herzog, R.W., Elder, M.E., Collins, S.W., Conlon, T.J., Clement, N., Cleaver, B.D., et al. (2011). Pompe disease gene therapy. Hum. Mol. Genet. 20 (R1), R61–R68.

69. Banugaria, S.G., Prater, S.N., Ng, Y.K., Kobori, J.A., Finkel, R.S., Ladda, R.L., Chen, Y.T., Rosenberg, A.S., and Kishnani, P.S. (2011). The impact of antibodies on clinical outcomes in diseases treated with therapeutic protein: lessons learned from infantile Pompe disease. Genet. Med. 13, 729–736.

70. van Gelder, C.M., Hoogeveen-Westerveld, M., Kroos, M.A., Plug, I., van der Ploeg, A.T., and Reuser, A.J. (2015). Enzyme therapy and immune response in relation to

CRIM status: the Dutch experience in classic infantile Pompe disease. J. Inherit. Metab. Dis. *38*, 305–314.

71. Sun, B., Zhang, H., Bird, A., Li, S., Young, S.P., and Koeberl, D.D. (2009). Impaired clearance of accumulated lysosomal glycogen in advanced Pompe disease despite high-level vector-mediated transgene expression. J. Gene Med. *11*, 913–920.

72. Franco, L.M., Sun, B., Yang, X., Bird, A., Zhang, H., Schneider, A., Brown, T., Young, S.P., Clay, T.M., Amalfitano, A., et al. (2005). Evasion of immune responses to introduced human acid alpha-glucosidase by liver-restricted expression in glycogen storage disease type II. Mol. Ther. *12*, 876–884.

73. Zhang, P., Sun, B., Osada, T., Rodriguiz, R., Yang, X.Y., Luo, X., Kemper, A.R., Clay, T.M., and Koeberl, D.D. (2012). Immunodominant liver-specific expression suppresses transgene-directed immune responses in murine pompe disease. Hum. Gene Ther. *23*, 460–472.

74. Sun, B., Chen, Y.T., Bird, A., Xu, F., Hou, Y.X., Amalfitano, A., and Koeberl, D.D. (2003). Packaging of an AAV vector encoding human acid alpha-glucosidase for gene therapy in glycogen storage disease type II with a modified hybrid adenovirus-AAV vector. Mol. Ther. *7*, 467–477.

75. Lock, M., Alvira, M., Vandenberghe, L.H., Samanta, A., Toelen, J., Debyser, Z., and Wilson, J.M. (2010). Rapid, simple, and versatile manufacturing of recombinant adeno-associated viral vectors at scale. Hum. Gene Ther. *21*, 1259–1271.

76. Raben, N., Nagaraju, K., Lee, E., Kessler, P., Byrne, B., Lee, L., LaMarca, M., King, C., Ward, J., Sauer, B., and Plotz, P. (1998). Targeted disruption of the acid alpha-glucosidase gene in mice causes an illness with critical features of both infantile and adult human glycogen storage disease type II. J. Biol. Chem. *273*, 19086–19092.

77. Lynch, C.M., Johnson, J., Vaccaro, C., and Thurberg, B.L. (2005). High-resolution light microscopy (HRLM) and digital analysis of Pompe disease pathology. J. Histochem. Cytochem. *53*, 63–73.

78. Taksir, T.V., Griffiths, D., Johnson, J., Ryan, S., Shihabuddin, L.S., and Thurberg, B.L. (2007). Optimized preservation of CNS morphology for the identification of glycogen in the Pompe mouse model. J. Histochem. Cytochem. *55*, 991–998.

79. Galjaard, H., Mekes, M., Josselin de Jong JE, D.E., and Niermeijer, M.F. (1973). A method for rapid prenatal diagnosis of glycogenosis II (Pompe's disease). Clin. Chim. Acta *49*, 361–375.

80. Raben, N., Shea, L., Hill, V., and Plotz, P. (2009). Monitoring autophagy in lysosomal storage disorders. Methods Enzymol. *453*, 417–449.

81. Chaplan, S.R., Bach, F.W., Pogrel, J.W., Chung, J.M., and Yaksh, T.L. (1994). Quantitative assessment of tactile allodynia in the rat paw. J. Neurosci. Methods *53*, 55–63.

82. Luong, T.N., Carlisle, H.J., Southwell, A., and Patterson, P.H. (2011). Assessment of motor balance and coordination in mice using the balance beam. J. Vis. Exp. (49), 2376.

83. Heck, D.H., Zhao, Y., Roy, S., LeDoux, M.S., and Reiter, L.T. (2008). Analysis of cerebellar function in Ube3a-deficient mice reveals novel genotype-specific behaviors. Hum. Mol. Genet. *17*, 2181–2189.

84. Leger, M., Quiedeville, A., Bouet, V., Haelewyn, B., Boulouard, M., Schumann-Bard, P., and Freret, T. (2013). Object recognition test in mice. Nat. Protoc. *8*, 2531–2537.

85. Fukuda, T., Ahearn, M., Roberts, A., Mattaliano, R.J., Zaal, K., Ralston, E., Plotz, P.H., and Raben, N. (2006). Autophagy and mistargeting of therapeutic enzyme in skeletal muscle in Pompe disease. Mol. Ther. *14*, 831–839.

86. Douillard-Guilloux, G., Raben, N., Takikita, S., Ferry, A., Vignaud, A., Guillet-Deniau, I., Favier, M., Thurberg, B.L., Roach, P.J., Caillaud, C., and Richard, E. (2010). Restoration of muscle functionality by genetic suppression of glycogen synthesis in a murine model of Pompe disease. Hum. Mol. Genet. *19*, 684–696.

87. Xu, S., Galperin, M., Melvin, G., Horowits, R., Raben, N., Plotz, P., and Yu, L. (2010). Impaired organization and function of myofilaments in single muscle fibers from a mouse model of Pompe disease. J. Appl. Physiol. *108*, 1383–1388.